Applied Energy 357 (2024) 122473

Contents lists available at ScienceDirect

Applied Energy

journal homepage: www.elsevier.com/locate/apenergy

Innovative approaches for deep decarbonization of data centers and building space heating networks: Modeling and comparison of novel waste heat recovery systems for liquid cooling systems

Tao Lu [a], Xiaoshu Lü [a,b,*], Petri Välisuo [a], Qunli Zhang [c], Derek Clements-Croome [d]

[a] Department of Electrical Engineering and Energy Technology, University of Vaasa, P.O. Box 700, FIN-65101 Vaasa, Finland
[b] Department of Civil Engineering, Aalto University, P.O. Box 11000, 02150 Espoo, Finland
[c] Beijing Key Lab of Heating, Gas Supply, Ventilating and Air Conditioning Engineering, Beijing University of Civil Engineering and Architecture, Beijing 100044, China
[d] School of Built Environment, University of Reading, PO Box 219, Reading RG6 6AW, UK

HIGHLIGHTS

- Non-heat pump data center waste heat recovery for space heating is studied.
- Two schemes, recovering from both sides of cooling distribution unit, are compared.
- The two schemes achieve payback in under a year due to the elimination of heat pump.
- Waste heat recovery on the secondary side outperforms that on the primary side.
- Novel relationship graphs facilitate data center waste heat recovery system design.

ARTICLE INFO

Keywords:
Data center waste heat utilization
Liquid-cooled rack
District heating networks
Building space heating
Life cycle cost
Life cycle CO_2 emission reduction

ABSTRACT

The data usage surge drives greater data center demand, amplifying global CO_2 emissions. Mitigating climate change necessitates reducing data center CO_2 emissions. Reusing waste heat from data centers offers a potential energy efficiency boost and environmental impact reduction. This study utilizes liquid cooling technology to raise waste heat temperature for building space heating and introduces the concept of 'data furnaces,' where data centers directly supply waste heat to heat buildings on-site, reducing district heating consumption and lowering CO_2 emissions. Efficiently designing a heat recovery heat exchanger system that accounts for both heat rejection and cooling sides of a liquid cooling system is crucial for achieving complete heat recovery without using heat pump, a commonly overlooked aspect in existing literature. To address this issue, we propose two heat exchanger schemes: connecting the building space heating network to the secondary side (Scheme 1) and the primary side (Scheme 2) of the cooling distribution unit. Implementing these innovations leads to the elimination of dependence on a heat pump, substantially cutting energy and CO_2 emissions. Using TRNSYS software, we develop, model, and compare waste heat recovery schemes to curb district heating consumption and CO_2 emissions. To demonstrate broad implications of the proposed approaches for energy efficiency and sustainability in the data centers and building space heating networks, a showcase study examines constant 25 kW waste heat from a direct-to-chip liquid-cooled rack in an office building with 285.7 MWh annual space heating demand. A novel waste heat recovery rate relationship graph is created to assist system design, uncovering an unexpected result in Scheme 2: waste heat recovery decreases as outdoor temperature falls. In contrast, Scheme 1 maintains a stable waste heat recovery rate around 25 kW, regardless of outdoor temperature fluctuations. As a result, Scheme 1 reuses 155.2 MWh of waste heat annually compared to 138 MWh for Scheme 2. Schemes 1 and 2 yield annual electricity savings of 2290.5 kWh and 905.2 kWh, respectively, for the cooling system. Both schemes achieve profitability within a year through a 25-year life cycle analysis (LCC) and substantially reduce CO_2 emissions, with Scheme 1 saving 291,996 $kgCO_2$ and Scheme 2 saving 258,192 $kgCO_2$. The study addresses critical gaps in existing literature by emphasizes LCC. The proposed heat exchanger designs represent pioneering solutions for optimizing waste heat recovery, particularly in challenging climates. New findings offer substantial benefits to

* Corresponding author at: Department of Electrical Engineering and Energy Technology, University of Vaasa, P.O. Box 700, FIN-65101 Vaasa, Finland.
E-mail address: xiaoshu.lu@aalto.fi (X. Lü).

https://doi.org/10.1016/j.apenergy.2023.122473
Received 16 August 2023; Received in revised form 7 November 2023; Accepted 4 December 2023
Available online 15 December 2023

both liquid-cooled and air-cooled facilities, making significant contributions to achieve carbon neutrality in data center operations.

Nomenclature

C_0	initial investment cost in euros (€)
C_n	annual cash flow in euros (€)
$C_{coolant}$	coolant heat capacity rate (kW/^{o}C)
C_{sp}	water heat capacity rate (kW/^{o}C) in the secondary side of the space heating network
C_n^{DH}	cost savings associated with district heating (€)
$C_n^{maintainance}$	maintenance cost related to C_n^{DH}(€)
$CO_2emssion_{reduction}$	annual reduction in CO_2 emissions
$\dot{m}_{bypassing\_source\_side\_HX2}$	mass flow rate of waste heat bypassing HX2 (kg/s)
$\dot{m}_{entering\_source\_side\_HX2}$	mass flow rate of waste heat entering HX2 (kg/s)
N	total number of years
$\dot{P}_{fan}$	fan power (kW)
$\dot{P}_{fan,rated}$	rated fan power (kW)
$q_{servers}$	power dissipated by servers = 25 kW
q_{sp}	space heating power (kWh)
$Q_{DH\_electricity\_saving}$	saved district heating energy and electricity (including the dry cooler and the pump in the primary side of CDU) (kWh)
Q_{sp}	annual space heating power (kWh)
r	discount rate
S_{HDD}	heating degree day (Kh or ^{o}Ch)
$t_{timestep}$	time step (h)
T_{HDD}	indoor HDD temperature = 17 °C
T_o	outdoor temperature (°C)
T_{rack_inlet}	rack inlet coolant temperature (°C)
T_{rack_outlet}	rack outlet coolant temperature (°C)
$T_{sp_{return}}$	space heating return water temperature(°C)
$T_{sp_{supply}}$	space heating supply water temperatures (°C)
γ	ratio of the current fan speed to the design fan speed
ε	emission factor in kilograms of CO_2 per kilowatt-hour ($kgCO_2$/kWh)

Abbreviations

AC	alternating current
CDU	cooling distribution unit
CDU_HX	liquid-to-liquid heat exchanger in the cooling distribution unit
CO_2	carbon dioxide
CRAC	computer room air conditioner
CRAH	computer room air handling
DH	district heating
HDD	heating degree day
HX	heat exchanger
HX2	heat recovery liquid-to-liquid heat exchanger
LCC	life cycle cost
NPV	net present value
ORC	organic Rankine cycle
RES	renewable energy sources
UA	overall heat transfer coefficient
WSTAR	Wasa Zero Emission Data Centre (project name)

1. Introduction

Due to the exponential growth in data usage, there has been a significant surge in demand for data centers and, consequently, their electricity consumption. According to the International Energy Agency (IEA) [1], data centers accounted for approximately 1–1.5% of global electricity consumption and emitted 300 Mt. CO_2-eq in 2020, which represents about 0.9% of energy-related greenhouse gas (GHG) emissions, the same as airline industry. To address the urgent need to combat climate change, each country has formulated its own climate policy. Finland, for instance, has set a target to become carbon-neutral and the first fossil-free welfare society by 2035 [2]. Hence it is crucial to reduce CO_2 emissions from data centers and ensure their green operation [3].

Statistics reveal that over 30% of the total energy consumed by data centers is allocated to cooling purposes. This indispensable cooling operation is essential to maintain optimal temperatures for the efficient functioning of the intricate network of servers and equipment. An alarming consequence of this cooling process is that the overwhelming majority of the consumed electricity by data centers, including cooling operations, is ultimately dissipated as heat, often dissipating into the atmosphere without any productive use. This inefficiency highlights the pressing need for innovative approaches and sustainable technologies to mitigate the waste energy of valuable resources while ensuring the seamless operation of growing demand for energy by data centers. Harnessing this waste heat offers a viable solution to minimize energy wastage and mitigate the environmental impact. In particularly, utilizing waste heat generated during their operation for building heating purposes can significantly enhance the energy efficiency and environmental sustainability of data centers [4,5] because, globally, buildings are responsible for about 40% of the total energy consumption and 36% of greenhouse gas emissions. In the EU, over 75% energy used in heating is from fossil fuel in building sector [6]. District heating (DH) networks have garnered attention as an efficient means of curbing building energy consumption and reducing CO_2 emissions, particularly in the Nordic countries. In Finland for instance, over half of the population relies on district heating systems for building heating [7]. However, a substantial portion of district heating systems across the globe still heavily relies on fossil fuels for heat production, thereby limiting the extent of its environmental benefits. The CO_2 emission coefficient (gCO_2/kWh) associated with DH has been higher than that of electricity in Finland [8], and this trend is expected to persist in the future [9]. On a global scale, DH contributed to 3.5% of CO_2 emissions in 2021, marking a 3.5% increase from the previous year [1]. These statistics emphasize the pressing necessity to lower CO_2 emissions from DH and buildings. In light of the research findings aiming to optimize future buildings, reducing or eliminating fossil fuel combustion [10]. Two main perspectives emerged: One foresees low-energy buildings eradicating heating needs, while the other suggests utilizing excess heat from industries, waste incineration, and power stations, along with geothermal energy, solar thermal systems, and heat pumps, to harness wind energy for heating buildings [10]. In the first scenario, DH networks become unnecessary; in the second, they are crucial. In both cases, eliminating DH networks or reducing CO_2 emissions from DH networks becomes a key global energy policy imperative.

Research and innovations related to the second scenario, focusing on reducing CO_2 emissions from DH networks, have been extensively explored by many researchers [10,11]. While many papers address renewable energy sources (RES) and fossil fuel substitution by RES, the importance of reusing data center waste heat for DH is underscored [5]. In the context of the first scenario, given the substantial presence of existing buildings with long lifespans and the expansion of distributed and edge data centers in many years ahead, direct data center waste heat utilization for building heating could make a substantial contribution to reducing CO_2 emissions. Regrettably, this research topic has been largely disregarded. Additional insights will be presented in the subsequent discussion.

One common and popular method for reducing CO_2 emissions from DH networks is to channel the waste heat generated from data centers into local DH networks [5]. This approach offers a clear advantage by allowing the full utilization of data center waste heat even during the summer months, thereby maximizing reductions in CO_2 emissions directly. It has gained recognition and popularity, particularly in Nordic countries like Finland, known for its tradition and leadership in reusing data center waste heat in DH networks. In 2010, a Helsinki-based energy company and Finnish IT Academica collaborated to build a 2 MW data center within an underground bomb shelter from the Second World War [12]. This data center employs Baltic sea water for cooling and transfers its waste heat to the local DH network via a heat pump, which can provide heating for approximately 1000 apartments. Additionally, Telia, a Nordic telecom operator, constructed the largest colocation data center in the Nordic countries in Helsinki in 2019 [13]. Since 2022, the waste heat from this data center has been collected by the energy company Helen for its DH network, which is capable of providing heating for over 20,000 dwellings. Expanding upon this trend, Microsoft has announced plans to build a data center in the Finnish cities of Espoo and Kirkkonummi [14]. The Finnish energy company Fortum will invest in the heat recovery project for the Microsoft data center, aiming to supply approximately 40% of the two cities' district heat. This project is regarded as the world's largest data center heat recovery initiative, expected to reduce annual CO_2 emissions by 400,000 tons. Furthermore, several research studies have contributed to addressing this issue.

Oró et al. [15] analyzed the economic feasibility of selling waste heat generated by a 1000 kW air-cooled data center, utilizing two distinct cooling technologies (computer room air handling (CRAH), chiller and rear door technology), to a local DH network in Spain. They evaluated two heat recovery solutions, namely heat recovery from the return hot aisle and heat recovery from the chiller condenser, under different operational scenarios. The results indicated that not all scenarios were economically viable, with heat recovery from the return hot aisle using an air-to-water heat exchanger proving to be the most economically feasible, with a payback period ranging between 10 and 14 years. On the other hand, heat recovery from the chiller condenser generally resulted in payback periods exceeding 15 years. Oltmanns et al. [16] presented two concepts for reusing waste heat generated by a high-performance computing (HPC) data center (360 kW) cooled by hot water. The data center was located within a university. The first concept involved transferring the data center waste heat to the return line of the campus DH network through a heat pump, resulting in an approximate 5 °C increase in the return line temperature. The second concept directly utilized data center waste heat for heating nearby buildings on the campus without a heat pump. In this approach, the waste heat was utilized to supply the ceiling panels of buildings at a temperature of 43 °C, while the radiators were still supplied with heat from the DH network. The simulations were performed using IDA software. The results revealed that approximately 50% of the waste heat could be reused annually in the first concept, while the second concept achieved a reuse rate of only 20%. The lower utilization rate in the second case was due to the buildings' heating demand being lower than the quantity of waste heat generated by the data center. Additionally, the capacity of the campus DH network was limited, which is the primary reason for incomplete extraction of data center waste heat in the first concept. Comparing the two concepts to the use of district heating alone, they resulted in yearly reductions of 720 tCO_2 and 570 tCO_2.

Directly utilizing data center waste heat for building heating often entails supplying heat to nearby buildings to reduce or eliminate DH and fossil fuel consumption [16–20]. Deymi-Dashtebayaz et al. [21] proposed an innovative system that combines free cooling and waste heat recovery to reduce both the cooling energy consumption of a data center in Iran while simultaneously reducing natural gas fuel consumption of a nearby office building. In this setup, the data center relied on a computer room air conditioner (CRAC) for cooling. To facilitate free cooling, two types of economizers were adopted: the air-side economizer and the water-side economizer. Furthermore, the return air from the server racks was captured to heat the nearby office building using an air source heat pump. This study conducted a comprehensive analysis from both a thermoeconomic and environmental perspective, considering four distinct system configurations, the air-side economizer, the water-side economizer, air source heat pump, and the combined setup of them. In terms of waste heat reuse, the results demonstrated that by employing an air source heat pump as a waste heat recovery system, the office building's natural gas consumption could be reduced by up to 15,000 cubic meters annually. Moreover, it is worth noting that various other studies have delved into systems that integrate cooling, heating, and electricity generation for data centers. Norani and Deymi-Dashtebayaz [22] introduced a comprehensive combined cooling, heating, and power system that encompassed an internal combustion engine, an organic Rankine cycle (ORC), and an absorption chiller. In this system, the internal combustion engine generated electricity to power a 1120 kW data center, and its waste heat was efficiently harnessed to drive the ORC and absorption chiller systems, thereby supplying both electricity and cooling to the data center. In a similar vein, Alipour et al. [23] proposed a co-generation system that combined the ORC, absorption chiller, and a linear parabolic collector. This innovative system had the capacity to simultaneously generate cooling, heating, and power. It operated by reusing the hot fluid from the evaporator of the ORC system as a heat source to drive the absorption chiller system, providing cooling for a 313 kW data center. The heat released from the absorption chiller system's generator was further enhanced using solar energy via the linear parabolic collector. This heated fluid was then used as a heat source to drive the ORC system, ultimately producing power for the data center. It should be underscored that while the focus of both studies [22,23] primarily revolved around cooling and electricity generation for data centers through the utilization of waste heat, rather than direct waste heat reuse for heating purposes, they introduced effective waste heat recovery technologies that could also prove beneficial for data center waste heat reuse in heating applications.

The data center heat recovery systems discussed in the studies above fall into two primary categories: those utilizing heat pumps to recover waste heat from data centers for utilization in district heating networks or buildings, and those relying solely on heat exchangers. These studies conducted comprehensive analyses, taking into account energy, economic, and environmental factors. The results indicate notable savings in heating energy and reductions in CO_2 emissions and costs to a certain extent. It is essential to emphasize that a significant portion of these studies focuses on heat pump waste heat recovery systems. The key advantage of these studies lies in their ability to provide the desired heating temperatures and maximize the utilization of waste heat. This versatility makes them well-suited for a wide range of heating applications, including district heating networks [15–17]. Conversely, waste heat recovery systems in data centers that do not incorporate heat pumps are not frequently addressed in these studies. This is mainly due to the fact that passive systems of this nature often require a high waste heat temperature for effective operation.

Due to the rapid increase in server power densities, liquid cooling technologies have gained popularity. Particularly the direct-to-chip cooling method employs cold plate technology to cool high-heat electronic components such as CPUs, GPUs, and memory modules [24–29]. A distinctive feature of direct-to-chip cooling is its ability to employ hot water as a coolant for server cooling [16,29], which is environmentally friendly. Direct-to-chip cooling can provide waste heat in the form of water at approximately 45 °C or even higher [16]. This temperature range corresponds to the maximum supply water temperature of some low temperature building heating systems. For example, it aligns with the specified maximum supply water temperature of 45 °C for space heating in the secondary side of building DH substations, as stated in the new regulations and guidelines for Finnish buildings [30]. This offers significant opportunities for utilizing waste heat from liquid-cooled racks for heating these low temperature buildings without relying on heat pump [16]. However, the literature contains only a limited number of related studies and most related research focuses on recovering waste heat from the primary side of the cooling distribution unit (CDU), where waste heat is dissipated into the environment [16,31]. Commercial liquid cooling products primarily provide access to the primary side for waste heat recovery. It is worth noting that waste heat can be recovered from either the primary side [16,31] or the secondary side. There is a lack of studies that explore the performance differences between waste heat recovery from the primary and secondary sides of a CDU especially concerning DH-based building space heating networks, which constitute substantial energy consumers within the building sector. This comparison is crucial for designing efficient heat recovery systems to minimize DH consumption. Our study, conducted as part of the WSTAR (Wasa Zero Emission Data Centre) project supported by the European Union's NextGenerationEU instrument and the Academy of Finland [32], aims to address this research gap.

In this study, we employ liquid-cooled racks within an office building as 'data furnaces' to supply heat to the return line of the secondary side of the space heating network. This innovative approach eliminates the need for a heat pump and reduces district heating demand and investment costs. Moreover, this setup minimizes heat loss from the pipes since they are enclosed within the building. Consequently, waste heat utilization has the potential to transform the data center into facilities with zero or even negative CO_2 emissions. The 'data furnaces' concept is innovative and aligns with the increasing demand for distributed and edge data centers due to advancements in cloud, distributed, and edge computing technologies [33,34]. These compact data centers can conveniently be located within office or residential buildings, effectively functioning as data furnaces. The idea is to integrate data centers into these buildings, enabling the direct harnessing of waste heat for heating purposes [35]. Furthermore, we have developed a novel relationship graph using scatter plots to illustrate the connection between waste heat recovery rate and outdoor temperature. This novel graph facilitates the design of waste heat recovery systems for DH-based building space heating networks. Given that the supply water temperature of such networks is linearly correlated with outdoor temperature, utilizing these graphs enables the straightforward identification of the most efficient design from a set of options. In an ideal scenario, the relationship graph of a design should exhibit no correlation between waste heat recovery rate and outdoor temperature throughout the heating season, signifying complete waste heat recovery. These graphs represent additional innovations in our study. The objectives of this study are:

- To develop different connection schemes for recovering data center waste heat from either the primary or secondary side of the CDU using a liquid-to-liquid heat exchanger.
- To model and evaluate the performance of the developed connection schemes in terms of waste heat utilization employing the developed novel relationship graph, particularly under extremely cold weather conditions. The aim is to identify a connection scheme that is not affected by outdoor temperature fluctuations, ensuring consistent waste heat utilization performance. To simplify the study, we assume the effectiveness of the heat recovery heat exchanger is the same as that of the CDU heat exchanger, determined from experimental data in the literature. This approach ensures a realistic and informative study that avoids the need to analyze the effects of heat exchanger effectiveness on connection scheme performance, which is not essential for this study's objectives.
- To conduct a life cycle cost (LCC) and CO_2 emission reduction analysis for different connection schemes. Although the majority of the investment for the WSTAR data center comes from European Union and the Academy of Finland, we anticipate securing additional investment for the data center waste heat utilization system from the building owner where the data center will be situated. Therefore, all LCC analyses in this study consider the perspective of the building owner, and investment costs encompass only the equipment and devices necessary for the building's space heating network to utilize waste heat, such as liquid-to-liquid heat exchangers, pipework, and certain automation components.

In summary, this paper is dedicated to the development, modeling, and comparison of various waste heat recovery schemes that connect the secondary side of the building's space heating network with either the primary or the secondary side of the CDU. The primary goal is to optimize the utilization of data center waste heat, thereby reducing DH consumption and CO_2 emissions. This study addresses several gaps in the existing literature and serves as a valuable reference not only for liquid-cooled data centers but also for air-cooled data centers. It is worth noting that the LCC analysis is restricted to the data center waste heat utilization system, underlining the scope of this research.

2. Methodology

We demonstrate the proposed methods in the WSTAR pilot data center. This data center has a 50 kW capacity, with 30 kW dedicated to direct-to-chip cooling for a single rack and an additional 20 kW for free air cooling. It is assumed that a steady 25 kW heat is captured from the liquid-cooled 30 kW rack using direct-to-chip cooling. This means that the data center liquid cooling requirement and waste heat sustain a constant 25 kW. Given that the WSTAR data center will be dedicated to research purposes for at least the first year after its construction, it is feasible to maintain the 30 kW rack operating at a constant capacity. Multiple potential office buildings are being considered for the WSTAR data center, with floor areas ranging from 2000 to 12,000 m^2. Our preference is an office building with an area close to 3000 m^2, as such building sizes are predominant among the potential options. It is important to highlight that the novel heat exchanger connection schemes developed in this paper for data center waste heat recovery can be applied to office buildings of various sizes.

In the absence of a heat pump, there are essentially two kinds of heat exchanger connection schemes for recovering waste heat from the liquid-cooled data center: connecting the secondary side of the space heating network to either the primary side or the secondary side of the CDU via a liquid-to-liquid heat exchanger. Therefore, we propose three types of models: a standalone direct-to-chip cooling system, a standalone space heating network, and a combined system where the direct-to-chip cooling system and space heating network are linked by a heat recovery heat exchanger. The primary focus will be on the third type of model. The standalone direct-to-chip cooling system and standalone space heating network serve as the base case. In this study, energy savings and CO_2 emission reductions will be calculated by comparing the base case to the different connection schemes (e.g., third type of models). For example, the annual district heating consumption is assumed to be 286 MWh for the standalone space heating network (base case). If a connection scheme (third type of model) reduces the annual district heating consumption to 140 MWh by utilizing data center waste heat, the energy saving would amount to 146 MWh per year. The CO_2 emission reduction would be determined by multiplying the emission factor ($kgCO_2$/MWh) of district heating by the district heating saved (146 MWh). For all simulations including three types of mathematical models, we adopt a dynamic approach using the commercial software TRNSYS 18 with a time step set at 1 h. TRNSYS is a transient system simulation program widely employed in renewable energy engineering and building simulations [36]. The subsequent subsections will introduce the relevant physical equations and input data utilized for modeling these three types of models in TRNSYS 18.

2.1. Direct-to-chip cooling system and input data

Fig. 1 illustrates a typical direct-to-chip liquid cooling system.

The coolant distribution unit (CDU) distributes coolant to each liquid-cooled server unit through the rack manifold [37]. CDU has various configurations [38], and Fig. 1 presents a common configuration that includes a liquid-to-liquid heat exchanger (CDU_HX) for outdoor waste heat rejection, a reservoir, and a circulating pump.

The input data for CDU_HX and pumps in Fig. 1 are obtained from Asetek's report [39]. Appendix VI of [39] presents typical performance data for an 80 kW CDU, including total heat capture (approximately 80 kW), facility flow rate (primary side), server flow rate (secondary side), server supply coolant temperature, server return coolant temperature, facility supply water temperature, facility return water temperature, and server node temperatures. The mass flow rates of the pumps are determined by scaling down the values in [39] based on the ratio of the heat capture in [39] to the data center waste heat (i.e., 25 kW). The specific heat capacity of the coolant, a water-propylene glycol mixture, is estimated from Asetek's report [39]. The heat exchanger effectiveness of CDU_HX is assumed constant and determined from experimental data in [39]. The input data for the dry cooler are based on the Airedale product [40]. Table 1 presents the important input data for the standalone direct-to-chip liquid cooling system shown in Fig. 1.

The fans of the dry cooler in Table 1 are alternating current (AC) fans [39]. While the electronically commutated (EC) fans are more energy efficient, their power-speed relationship is nonlinear and requires manufacturer-provided performance data [41]. In contrast, AC fans generally exhibit a linear correlation between fan power and speed [41]. In this study, fan power ($\dot{P}_{fan}$) is calculated as

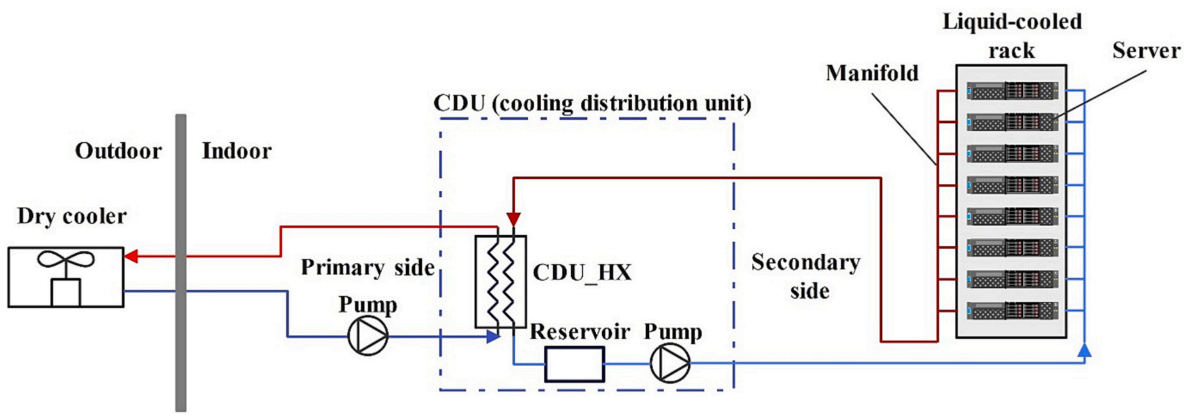

Fig. 1. Direct-to-chip liquid cooling system (base case).

Table 1
Input data for the standalone direct-to-chip cooling system.

CDU (coolant distribution unit)		
Heat exchanger (CDU_HX) effectiveness		0.7 (constant)
Pump	Mass flow rate (kg/h)	1000
	Input power (kW)	0.25
Coolant specific heat capacity (kJ/kg.°C)		3.91 (water mixed with propylene glycol)
Primary side		
Pump	Mass flow rate (kg/h)	1200
	Input power (kW)	0.25
Fluid specific heat capacity (kJ/kg. °C)		3.53 (water mixed with propylene glycol)
Dry cooler	Design inlet fluid flow rate (°C)	45
	Design outlet fluid temperature (°C)	40
	Specific heat capacity (kJ/kg°C)	3.53
	Design ambient air temperature (°C)	35
	Design air flow rate (kg/h)	33,768
	Total Heat of Rejection (kW)	30.8
	Rated fan power (kW)	1.76
	Desired outlet fluid temperature	31 °C, ambient temperature ≤ 26 °C; Outdoor temperature + 5 °C, ambient temperature > 26 °C.

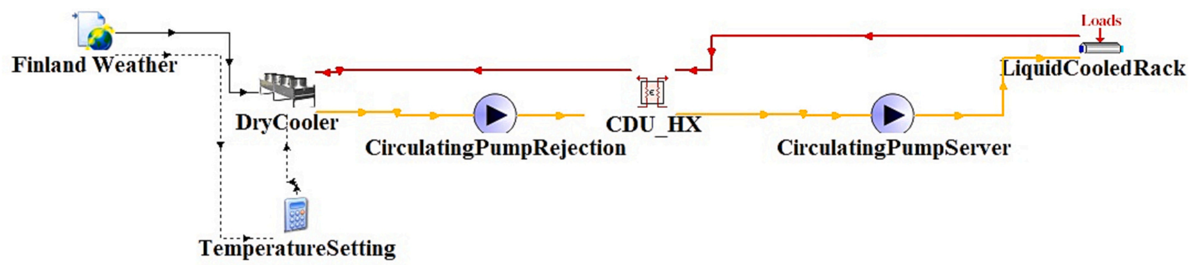

Fig. 2. TRNSYS model of the direct-to-chip cooling system (time step = 1 h).

$$\dot{P}_{fan} = \dot{P}_{fan,rated}\gamma \tag{1}$$

where $\dot{P}_{fan,rated}$ represents the rated fan power (kW) obtained from Table 1, and γ is the ratio of the current fan speed to the design fan speed. The rack outlet coolant temperature (T_{rack_outlet}) is determined as [42]:

$$T_{rack\_outlet} = T_{rack\_inlet} + \frac{q_{servers}}{C_{coolant}} \tag{2}$$

where T_{rack_inlet} is the rack inlet coolant temperature (°C), $q_{servers}$ is the power dissipated by servers (25 kW) and $C_{coolant}$ is the heat capacity rate of the coolant (kW/°C) (see Table 1). Note that a constant value 25 kW for $q_{servers}$ is assumed. In reality, $q_{servers}$ is influenced by the rack's inlet coolant temperature, T_{rack_inlet}, and is not a fixed constant. The experimental data utilized in this research is derived from Asetek's performance data for an 80 kW CDU [39]. According to the findings in [39], as the rack inlet coolant temperature rises from 30.3 °C to 40.77 °C, marking a 10.37 °C increase, the heat capture decreases from 70.278 kW to 67.931 kW. In simpler terms, the heat capture only decreases by approximately 3.4% when the rack inlet coolant temperature increases by 10.37 °C. As a result, our assumption of a constant $q_{servers}$ is justified in this study since variations in the rack inlet coolant temperature are expected to remain below 10 °C.

The reservoir is not considered in waste heat utilization modeling due to its insignificance. The implementation of the direct-to-chip cooling system (Fig. 1) using TRNSYS is depicted in Fig. 2.

The TemperatureSetting component (Equation) in Fig. 2 sets the desired outlet fluid temperature based on the outdoor temperature (the last row of Table 1). Eq. (2) is implemented in the LiquidCooledRack component (Type 682) in Fig. 2. The WSTAR data center is located in Vaasa, Finland (63°06′N 021°37′E). However, as TRNSYS lacks the weather data for Vaasa, Tampere (61°29′53″N 23°45′36″E), the third largest city in Finland, is selected as a weather location for the Finland Weather component (Type 15) in Fig. 2 due to its similar heating degree days with Vaasa.

Type 511 component (Dry Fluid Cooler) from the commercial software TRNSYS 18 [43] is employed to model the dry cooler. Type 511 characterizes the dry fluid cooler as a single-pass, cross-flow heat exchanger. Within Type 511, the overall heat transfer coefficient (UA) of the dry cooler is initially determined based on user-provided design data. This UA value is then adjusted according to current inlet conditions, which encompass fluid temperature, fluid flow rate, and outdoor temperature. Subsequently, the software calculates the necessary air flow rate for the dry fluid cooler to achieve a user-specified outlet liquid temperature [43]. It should be noted that Type 511 does not factor in wind speed and orientation in its calculations.

2.2. Building space heating network and input data

Fig. 3 depicts the space heating network employed in the university office building.

In accordance with the latest Finnish regulations and guidelines for buildings [30], the valve TV1 is utilized to regulate the flow rate of district heating through the source side of HX1 heat exchanger, which is contingent upon the outdoor temperature. This control mechanism ensures that the supply water temperature in the space heating network remains consistent with the predetermined value established by the control center. The regulations and guidelines [30] specify that the maximum supply water temperature for the space heating network should not exceed 45 °C, while the return water temperature should not surpass 30 °C. Therefore we assume that the control of the supply water temperature (TE1) in the space heating network is based on the control curve [44] in Fig. 4.

The specific details regarding the structural composition of the university office building are currently unknown. To effectively model the space heating network, we employ a steady-state model developed by VTT Technical Research Centre of Finland Ltd. [45]. This model facilitates the calculation of hourly space heating power ($q_{sp}(t)$) as follows:

$$q_{sp}(t) = \frac{Q_{sp}}{S_{HDD}}(T_{HDD} - T_o(t)), \text{when } T_{HDD} > T_o,$$

$$q_{sp}(t) = 0, \text{when } T_{HDD} \le T_o. \tag{3}$$

where Q_{sp} represents the annual space heating (kWh), S_{HDD} denotes the heating degree day (Kh or °Ch), T_{HDD} signifies the indoor temperature that represents the heating degree day in degrees Celsius (°C) and T_o represents the outdoor temperature (°C). Here T_{HDD} is set 17 °C. The

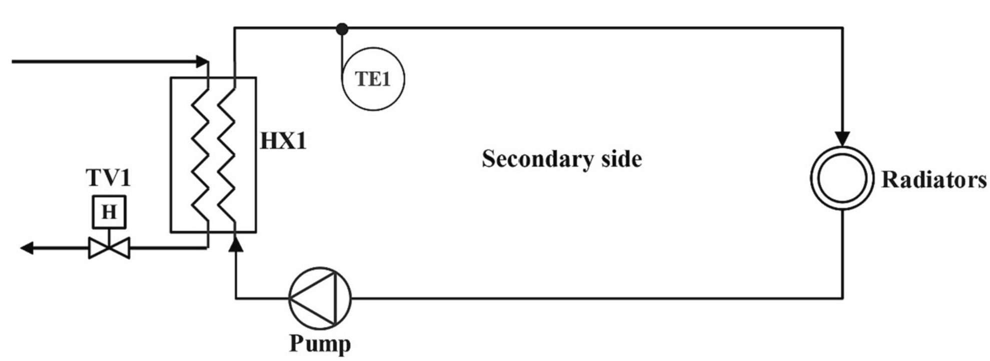

Fig. 3. Space heating network for the university office building (base case).

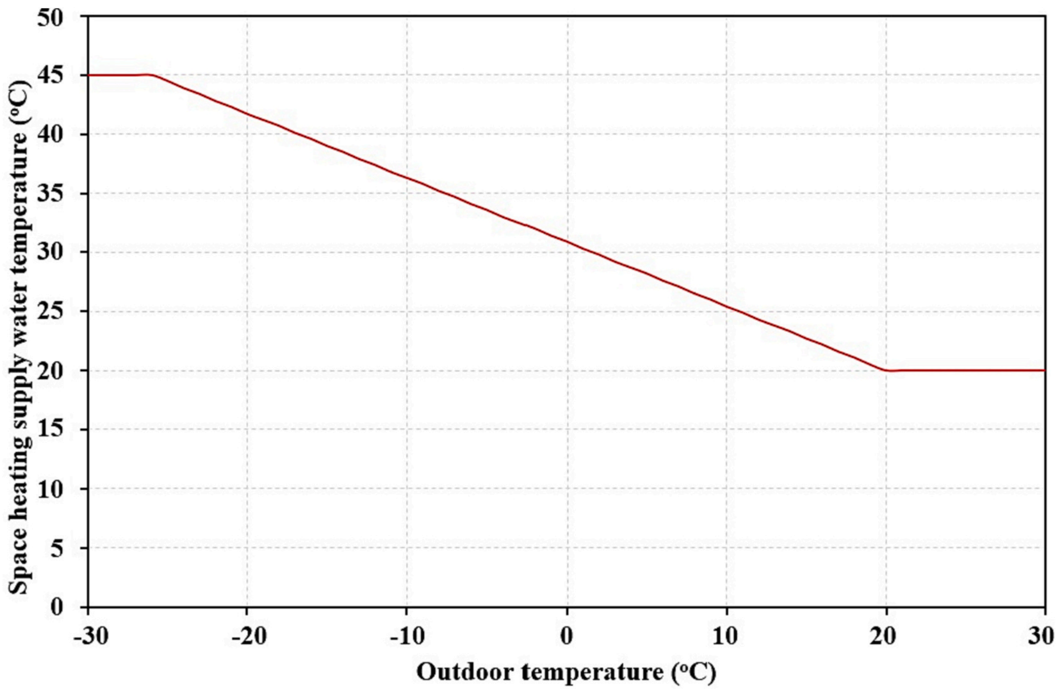

Fig. 4. Control curve for space heating supply water temperature [44].

heating degree day (S_{HDD}) is calculated as

$$S_{HDD} = \sum (T_{HDD} - T_o(t))t_{timestep} \tag{4}$$

where $t_{timestep}$ represents the time step (h). Specifically, for the Tampere weather conditions utilized in TRNSYS, the heating degree day is determined to be 119,509 Kh. Unfortunately, no information regarding the annual space heating consumption for the examined office building was available. However, in a separate Finnish city, Jyväskylä (62°14.5′N 025°44.5′E), the annual space heating consumption was estimated to be 105 kWh/m^2 for C1 type Finnish office buildings constructed between 1980 and 2000 [45]. Taking into account the heating degree days, this consumption value is adjusted to 96 kWh/m^2 for Tampere, resulting in an annual space heating consumption of the office building as 285,662 kWh. Furthermore, a water mass flow rate of 1.64 kg/s is assumed for the secondary side of the space heating network. Utilizing the provided information, the calculation of the space heating return water temperature ($T_{sp_{return}}(t)$) is determined as

$$T_{sp_{return}}(t) = T_{sp_{supply}}(t) - \frac{q_{sp}(t)}{C_{sp}} \tag{5}$$

where $T_{sp_{supply}}$ represents the space heating supply water temperatures (°C), and C_{sp} corresponds to the heat capacity rate of the water (kW/°C)

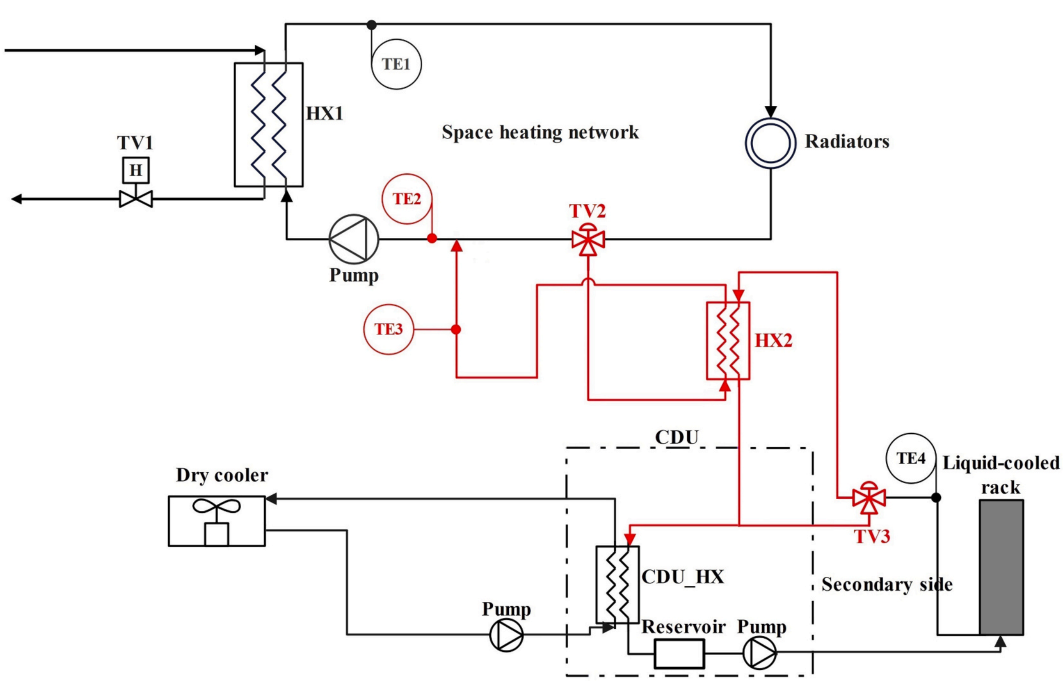

Fig. 5. Data center waste heat utilization network: Scheme 1.

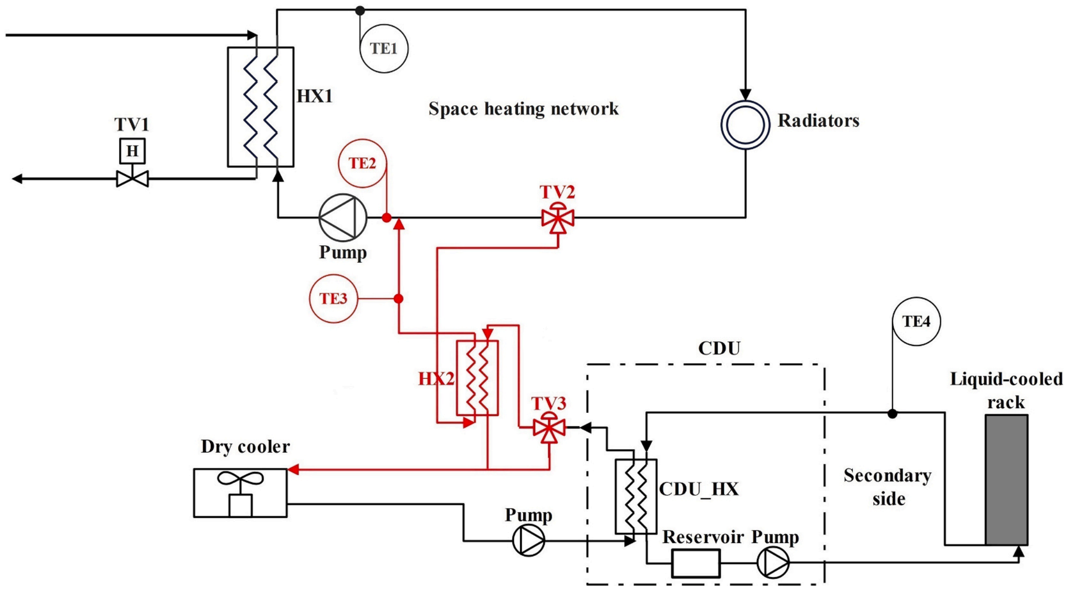

Fig. 6. Data center waste heat utilization network: Scheme 2.

in the secondary side of the space heating network (refer to Fig. 4). Eqs. (3)–(5) are programmed within TRNSYS' equation component, which will be elaborated on in the subsequent subsection.

2.3. Heat exchanger connection schemes for data center waste heat utilization

Two heat exchanger connection schemes are proposed and illustrated in Figs. 5 and 6.

The red-highlighted sections in both figures represent modifications to the pipe lines for the standalone direct-to-chip liquid cooling system (Fig. 1) or newly added pipe lines and equipment. The primary distinction between the two schemes lies in the placement of the newly added liquid-to-liquid heat exchanger, referred to as "HX2". In Scheme 1, HX2 is connected to the secondary side of the CDU. However, in Scheme 2, HX2 is connected to the primary side of the CDU. Scheme 1 can be regarded as utilizing the return water from the space heating network to directly cool the IT servers. If the waste heat cannot be fully utilized in Scheme 1, any remaining waste heat is then discharged to the outdoors through CDU_HX. In contrast to Scheme 2, where waste heat rejection and recovery are integrated within the same loop, Scheme 1 completely isolates waste heat rejection from the recovery process. Consequently, in Scheme 1, the pump in the primary side of the CDU can be stopped during cold winters since most of the waste heat is utilized. On the other hand, in Scheme 2, the pump must remain operational at all times. Clearly, this provides a notable advantage for Scheme 1.

HX2 (Figs. 5 and 6) serves as a heat recovery heat exchanger with the same effectiveness as the CDU_HX heat exchanger, i.e., 0.7. Commercial CDU products like Asetek [39], nVent [46], and CoolIT [47] typically offer liquid-to-liquid heat exchangers with effectiveness ranging from 0.5 to 0.8. Taddo [31] used an effectiveness of 0.7 for all liquid-to-liquid heat exchangers when modeling data center waste heat recovery systems using TRNSYS. Therefore, an effectiveness of 0.7 for the heat exchanger is a realistic value.

2.3.1. Mass flow rate controls

To maintain consistency, the mass flow rates of all pumps remain unchanged from those employed in the standalone direct-to-chip liquid cooling system and space heating network (Table 1). The mass flow rate of the space heating return water entering the load side of HX2 (depicted in Figs. 5 and 6) is held constant at 1200 kg/h by the three-way valve TV2. However, the source side mass flow rate of HX2 is regulated by the three-way valve TV3, utilizing an iterative feedback controller implemented in TRNSYS 18 as Type 22 [36]. Type 22 utilizes the secant method to calculate the control signal, minimizing tracking error. Further details about Type 22 can be found in [36]. The control strategies are outlined in the following:

- For outdoor temperature $\leq$ 6.55 °C, $\dot{m}_{entering\_source\_side\_HX2}$ equals 1000 kg/h for Scheme 1 and 1200 kg/h for Scheme 2, while $\dot{m}_{bypassing\_source\_side\_HX2}$ =0 for both. Here, $\dot{m}_{entering\_source\_side\_HX2}$ denotes the mass flow rate of waste heat entering HX2 from the direct-to-chip cooling system, and $\dot{m}_{bypassing\_source\_side\_HX2}$ indicates the mass flow rate of waste heat bypassing HX2.
- For 6.55 °C $<$ outdoor temperature $<$ 17 °C, the iterative feedback controller is activated to compute $\dot{m}_{entering\_source\_side\_HX2}$ for both schemes. $\dot{m}_{bypassing\_source\_side\_HX2}$ then equals $(1000\,kg/h - \dot{m}_{entering\_source\_side\_HX2})$ for Scheme 1 and $(1200\,kg/h - \dot{m}_{entering\_source\_side\_HX2})$ for Scheme 2.
- For outdoor temperature $\geq$ 17 °C, $\dot{m}_{entering\_source\_side\_HX2}$ equals 0 for both schemes, while $\dot{m}_{bypassing\_source\_side\_HX2}$= 1000 kg/h for Scheme 1 and 1200 kg/h for Scheme 2.

When the outdoor temperature is 6.55 °C, the space heating demand is approximately 25 kW. In essence, for both schemes, if the space heating demand equals or exceeds 25 kW (i.e., outdoor temperature $\leq$ 6.55 °C), the three-way valve TV3 is regulated to enable complete recovery of data center waste heat via the heat recovery heat exchanger HX2. Conversely, when the space heating demand is below 25 kW, an iterative feedback controller is utilized to regulate TV3, allowing only a portion of the data center waste heat to be recovered. This approach minimizes the difference between the space heating return water temperature (TE2) and the supply water temperature defined by the control curve presented in Fig. 4. In practical implementation, it may be necessary to modify this algorithm, as waste heat is unlikely to remain constant. For instance, the iterative feedback controller can be replaced with a proportional–integral–derivative (PID) controller, regulating TV3 to align the space heating return water temperature (TE2) as closely as possible with the space heating supply water temperature defined by the control curve in Fig. 4.

2.3.2. TRNSYS models

Two schemes are implemented using TRNSYS 18 [36] (Fig. 7 and Fig. 8).

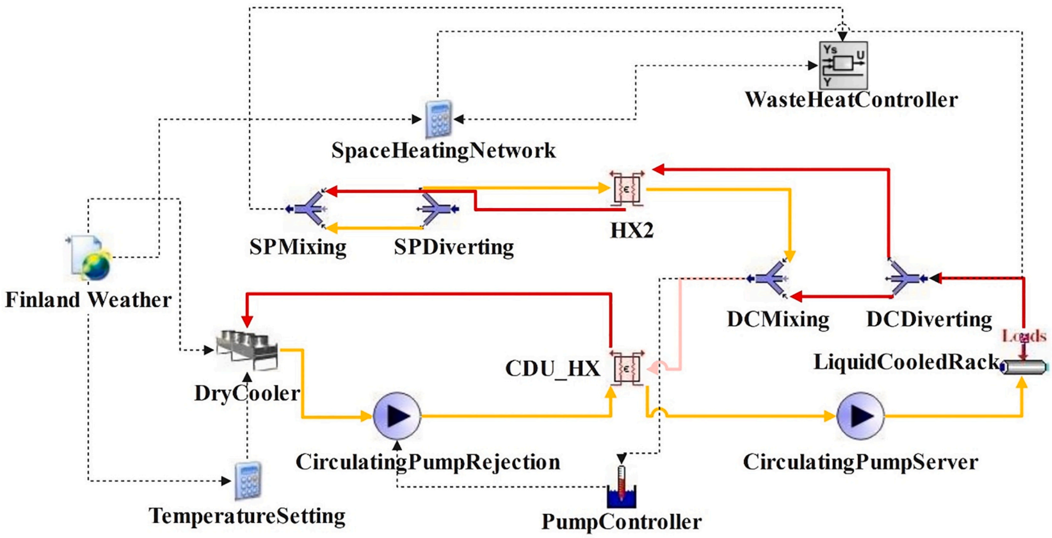

Fig. 7. TRNSYS model for Scheme 1 (time step = 1 h).

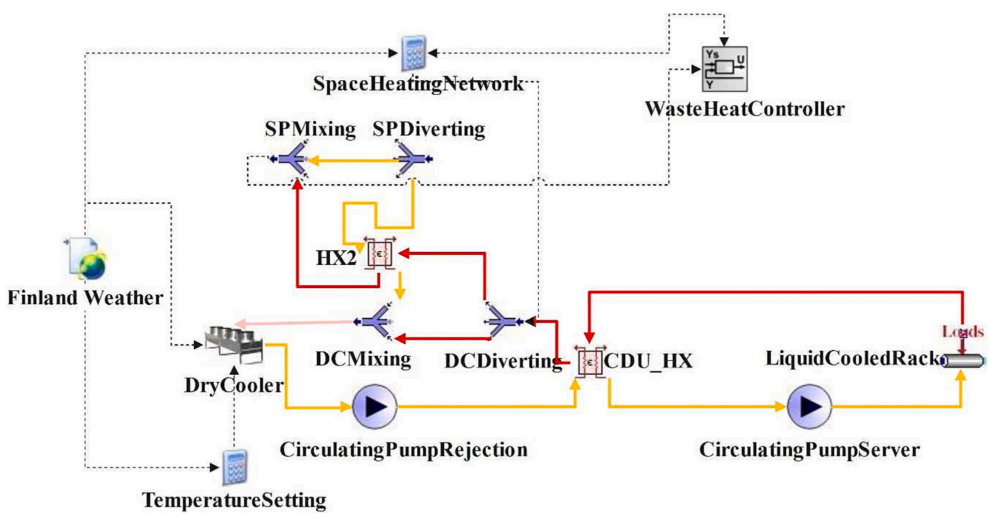

Fig. 8. TRNSYS model for Scheme 2 (time step = 1 h).

The SpaceHeatingNetwork component (Equation) incorporates the space heating network, including the control curve shown in Fig. 4 and Eqs. Eqs. (3) – (5). The three-way valves, TV2 and TV3, are simulated using the SPDiverting (Type 647), SPMixing (Type 649), DCDiverting (Type 647), and DCMixing (Type 649) components. The iterative feedback controller is modeled using the WasteHeatController component (Type 22). Additionally, in Scheme 1 (Fig. 7), a thermostat component named PumpController (Type 113) is utilized to activate the CirculatingPumpRejection (Type 114) only when the source side outlet temperature of CDU_HX exceeds 41 °C; otherwise, the pump remains inactive. This approach effectively saves pump energy, distinguishing it from Scheme 2, where the CirculatingPumpRejection needs to be operational at all times. In the subsequent analysis, we will examine this distinction along with the saved district heating for the two schemes.

2.4. Life cycle cost under euro and CO_2 emission reductions

The life cycle cost (LCC) assesses the profitability of different options by calculating the net present value (NPV) of the initial capital investment and all other life cycle costs. The NPV can be determined as [48].

$$NPV = -C_0 + \sum_{n=1}^{N} \frac{C_n}{(1+r)^n} \tag{6}$$

where C_0 represents the initial investment cost in euros (€), C_n denotes the annual cash flow in euros (€), N represents the total number of years, and r represents the discount rate. In this study, annual cash flow C_n is computed as

$$C_n = C_n^{DH} - C_n^{maintainance} \tag{7}$$

where C_n^{DH} corresponds to the cost savings associated with district heating, while $C_n^{maintainance}$ represents the maintenance cost related to C_n^{DH}. It is important to note that C_n^{DH} and $C_n^{maintainance}$ are inflation-adjusted costs, taking into account inflation to adjust the initial costs. The utilization of waste heat not only reduces the cost of district heating but also decreases the electricity expenses for the pump (e.g., in Scheme 1) and the dry cooler. As previously mentioned, the LCC analysis in this study is conducted from the perspective of the building owner rather than the data center owner. The electricity bill for the data center will be covered by the data center owner. Therefore, the electricity cost savings resulting from the pump in the primary side of the CDU and the dry cooler are not

Table 2
Investment cost components.

Components	Unit cost	Quantity (Scheme 1)	Quantity (Scheme 2)
Heating pipes	70.4 €/m	50	50
Plate heat exchanger	850 €	1	1
Actuated three-way valve	600 €	2	2
Siemens PLC (Programmable logic controller)	350 €	1	1
Waterproof DS18B20 digital temperature sensor	10 €	2	2
Wiring and connectors	40 €	1	1
Flow sensor	300 €	2	2
Total investment (€)		6570	6570
Installation cost (50% investment, €)		3285	3285
Capital cost (€)		9855	9855

included in the LCC assessment. However, these aspects will be addressed for both schemes in Section 3.

2.4.1. Investment cost

The primary cost associated with the heating system is attributed to the heating distribution pipes. As the specific location of the data center site has not been determined yet, an accurate estimation of pipe length is not available. For the purpose of analysis, we assumed a total pipe length of 50 m. Another significant cost factor is the installation cost. While some articles suggest that installation cost accounts for approximately 15% of the investment cost [49], in practice, it tends to exceed this percentage. When a project is entrusted to a company, the installation cost encompasses not only equipment delivery, installation, automation, and commissioning, but also project planning and supervision. In this study, we considered the installation cost to be approximately 50% of the investment cost. Table 2 provides a breakdown of the investment costs. All prices are derived from internet resources and are representative of average or above-average prices.

The annual maintenance cost is set at 2% of the total investment cost, resulting in a value of 131.4 € for both schemes. It should be noted that there may be additional costs associated with the purchase of a more powerful pump or an additional pump for the space heating network, considering the introduction of the data center waste heat network. However, these costs were not taken into account as the specific data center site has not been determined, and information regarding the pumps in the space heating network is currently unavailable. The input data required for the calculation of the net present value (NPV) are presented in Table 3.

Table 3
Input parameters for NPV.

Cost factor	Value
Number of years	25 [50]
Discount rate	7% [50]
Inflation rate	2% [51]
Electricity price for the first year	120.69 €/MWh [52]
Electricity inflation rate	2% [52]
District heating price for the first year	89.33 €/MWh [52]
District heating inflation rate	3% [52]

2.4.2. CO_2 emission reductions

The assumed district heating energy savings are kept constant for each year in both schemes. The annual reduction in CO_2 emissions can be calculated as

$$CO_2emssion_{reduction} = \varepsilon Q_{DH\_electricty\_saving} \tag{8}$$

where ε represents the emission factor in kilograms of CO_2 per kilowatt-hour (kgCO_2/kWh), and $Q_{DH\_electricity\_saving}$ corresponds to the saved district heating energy and electricity (including the dry cooler and the pump in the primary side of CDU) in kWh. The Finnish Ministry of the Environment has published emission factors for future years to assess the life cycle CO_2 emissions [53]. Fig. 9 illustrates the CO_2 emission factors for electricity and district heating over the calculated 25-year period.

3. Results and discussion

3.1. District heating and electricity savings by utilizing data center waste heat

Fig. 10 showcases the relationships between the recovered waste heat from the data center and the outdoor temperature during the coldest months of January and February.

In Scheme 2 (Fig. 10), the data center waste heat recovery rate decreases with outdoor temperature, dropping below 20 kW when the temperature is below −20 °C. In contrast, Scheme 1 maintains a stable waste heat recovery rate around 25 kW, regardless of outdoor temperature fluctuations. The primary reason for this discrepancy is the location difference of HX2. In Scheme 1, the data center waste heat is recovered through a single heat exchanger HX2, whereas the waste heat is recovered through two heat exchangers HX2 and CDU_HX in Scheme 2.

In the context of heat recovery using the liquid-to-liquid heat exchanger HX2, the maximum possible heat transfer rate is determined by the formula: $C_{liquid\_primary\_or\_secondary} * \left(T_{hot} - T_{sp_{return}}\right)$, where $C_{liquid\_primary\_or\_secondary}$ represents the liquid heat capacity rate (kW/^{o}C) on the secondary side of the CDU for Scheme 1 and on the primary side of the CDU for Scheme 2. In this equation, T_{hot} corresponds to the rack outlet coolant temperature for Scheme 1 and the outlet load temperature of the CDU for Scheme 2, as depicted in Figs. 5–6. $T_{sp_{return}}$ represents the temperature of the water returning from space heating. It is worth noting that the liquid's heat capacity rate on the secondary side of the CDU is slightly lower than that on the primary side. The difference is so small that can be disregarded for simplicity. Consequently, the maximum possible heat transfer rate is directly proportional to the temperature difference between the hot and cold fluids, namely $\left(T_{hot} - T_{sp_{return}}\right)$, for the heat recovery heat exchanger HX2. However, in the case of HX2 in Scheme 2, it is evident that the hot fluid's temperature (outlet load temperature of the CDU, as shown in Fig. 6) is lower than the rack outlet coolant temperature. This implies that the maximum possible heat transfer rate for Scheme 2 is smaller than that for Scheme 1. Simulation results confirm this observation. For instance, in January as depicted in Fig. 10, the average temperature difference between the hot and cold fluids for the heat recovery heat exchanger HX2 is 33.1 °C for Scheme 1 and only 27.09 °C for Scheme 2. This explains why Scheme 1 exhibits a more consistent and significant waste heat recovery rate compared to Scheme 2, as shown in Fig. 10. Even under extremely cold conditions, Scheme 1 still maintains a sufficiently large temperature difference for the heat recovery heat exchanger HX2 to fully recover waste heat generated by the data center. This also suggests that, in order to recover the same amount of data center waste heat, Scheme 1 requires

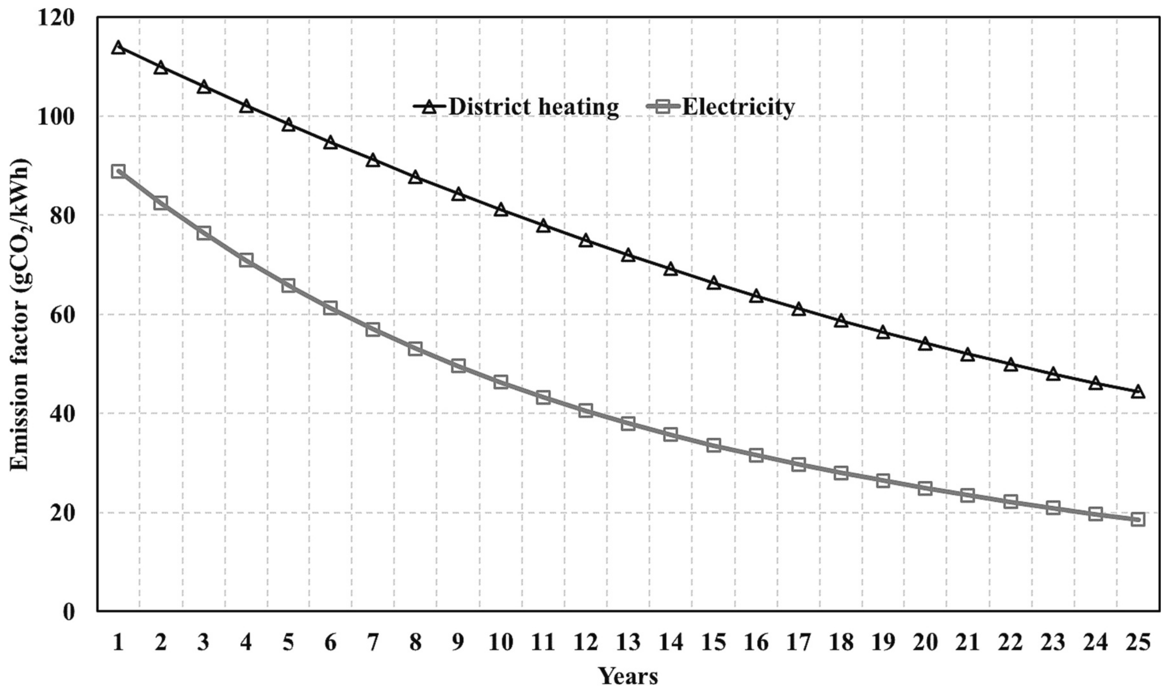

Fig. 9. CO_2 emission factors (gCO_2/kWh) [53].

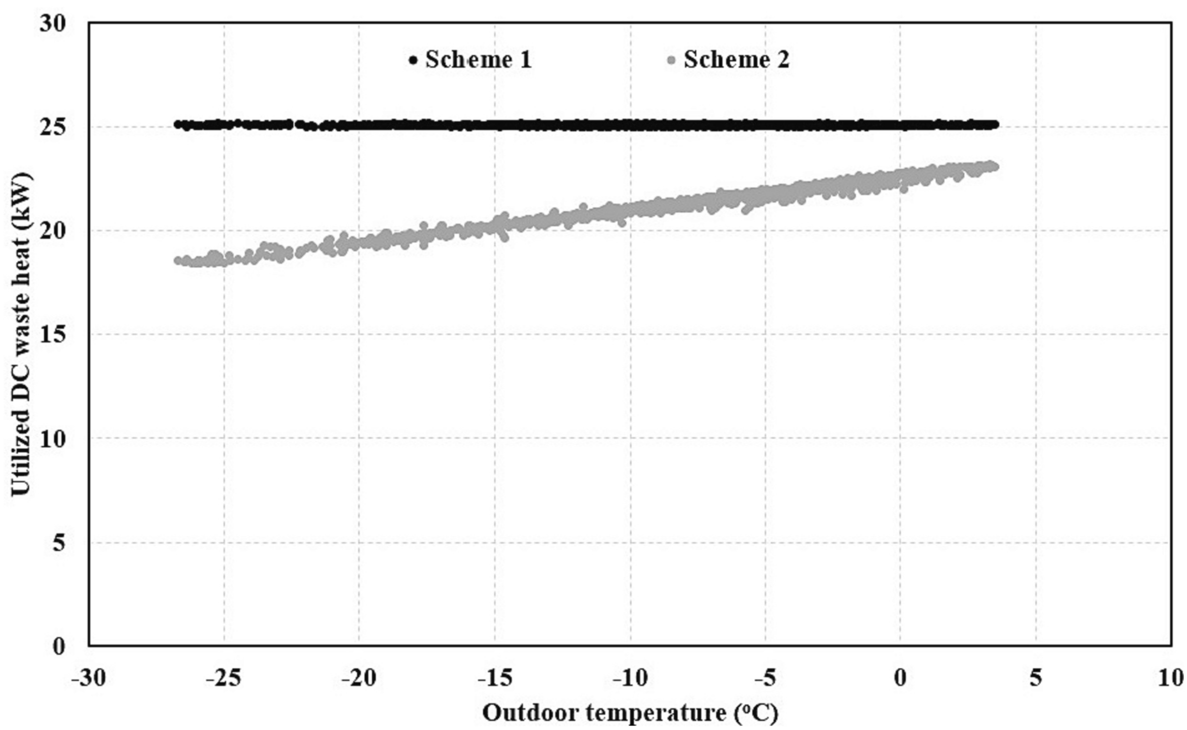

Fig. 10. Relationship between the recovered waste heat and outdoor temperature for the two schemes in January and February.

a lower waste heat temperature (TE4 in Figs. 5 and 6) compared to Scheme 2. A lower rack inlet coolant temperature generally implies a higher heat capture capability, as demonstrated in [39,47] in their CHx40 module cooling capacity performance graphs. In other words, Scheme 1 has the potential to recover more waste heat compared to Scheme 2. Another contributing factor is that the fluid temperature leaving the dry cooler is controlled around 31 °C to keep the rack inlet coolant temperature below 41 °C, in line with the experimental conditions in [39] to maintain waste heat close to 25 kW. As a result, in Scheme 2, the waste heat temperature is reduced, causing a minor portion of the waste heat to be expelled to the outdoors during periods of low outdoor temperature when the space heating return water temperature rises.

The above discussions offer scientific explanations for the differences in waste heat recovery rates between the two schemes, as depicted in Fig. 10. The resulting performance differences subsequently yield the flowing outcomes showcased in Figs. 11–12. Fig. 11 offers a monthly breakdown of waste heat utilization for both systems and Fig. 12

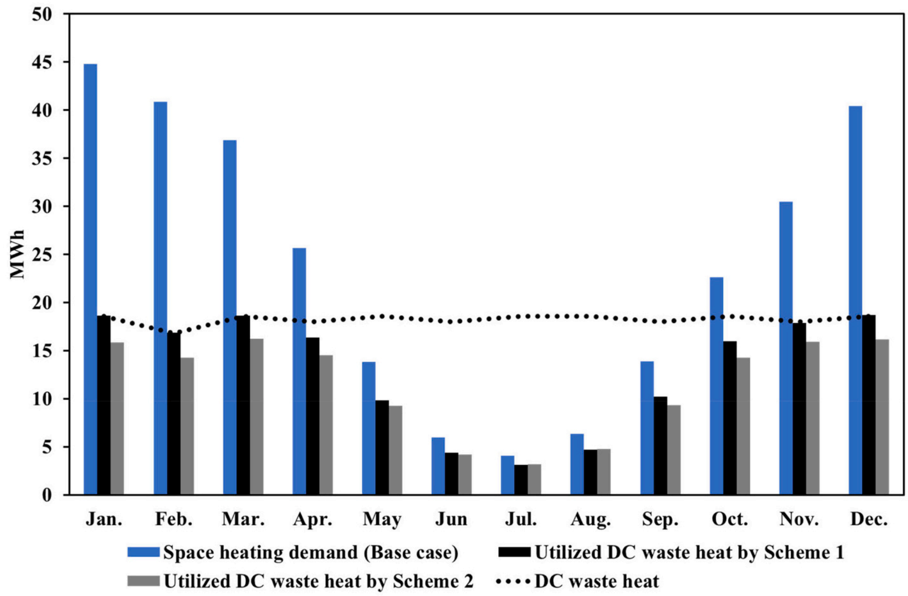

Fig. 11. Monthly utilized data center waste heat for the two schemes.

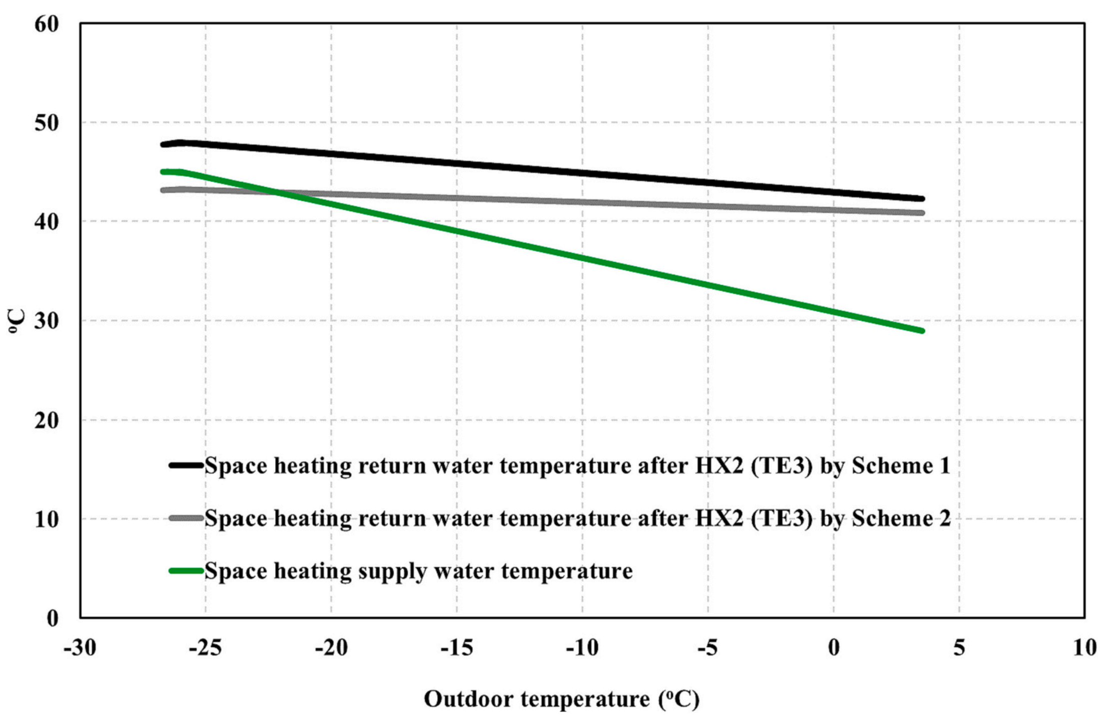

Fig. 12. Relationship between the load side outlet temperature of HX2 (TE3, Figs. 5 and 6) and outdoor temperature for the two schemes.

illustrates the correlation between the outlet temperature on the load side of HX2 (denoted as TE3 in Figs. 5 and 6) and outdoor temperatures during January and February:

- Scheme 1 outperforms Scheme 2 with an annual utilized waste heat of 155.2 MWh compared to 138 MWh for Scheme 2.
- During cold months of January, February, March, November, and December, almost all waste heat can be effectively reused in Scheme 1. Annually, approximately 71% and 63% of the waste heat can be utilized in Schemes 1 and 2, respectively.
- Scheme 1 can elevate the space heating return water temperature to the desired supply water temperature defined by the control curve in Fig. 4 without the need for a heat pump. In fact, even for Scheme 2, a heat pump is not required in the current case because district heating is still necessary during winter.

Notably in Fig. 11 when the space heating demand falls below the available waste heat (e.g., 25 kW), an iterative feedback controller (WasteHeatController in Figs. 7–8) activates to regulate the flow of waste heat into HX2 to ensure that it meets the current space heating demand. This control mechanism results in waste heat utilization fluctuating rather than precisely matching the space heating demand. During post-processing of the simulation data, all utilized waste heat data exceeding the space heating demand are considered equal to the

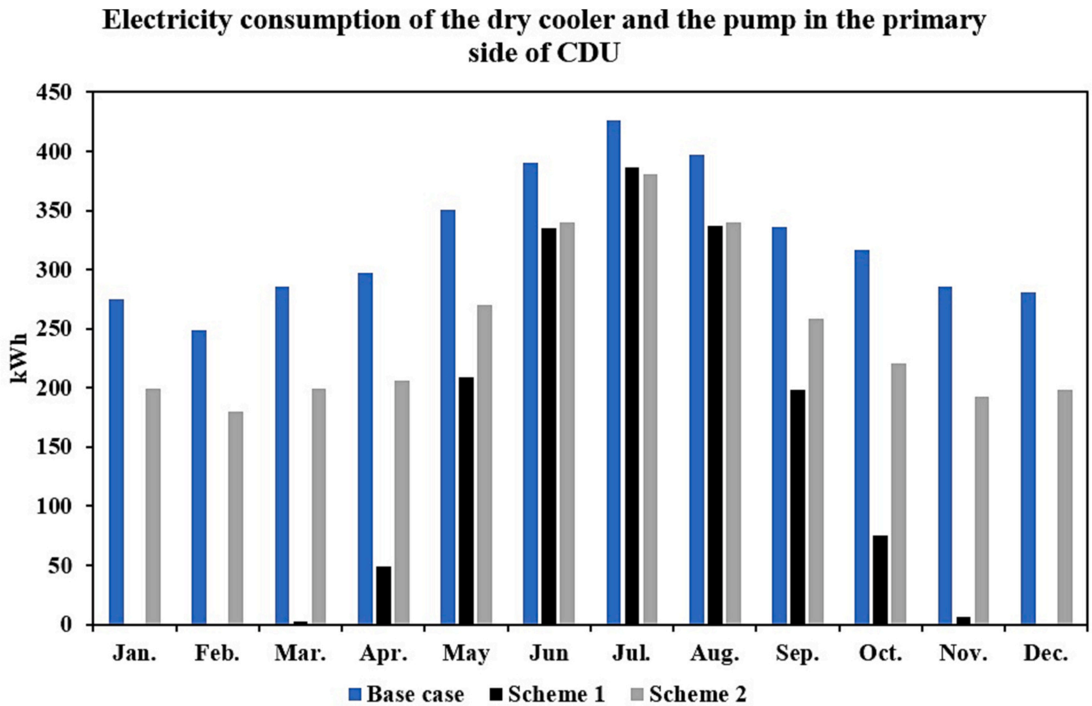

Fig. 13. Electricity consumption of the dry cooler and pump in the primary side of CDU for different cases.

space heating demand. Consequently, this leads to a slight discrepancy between the waste heat utilization data and the actual space heating demands in warmer months of June, July, and August.

In addition to the savings in district heating, the utilization of waste heat from the data center can also lead to reduced electricity consumption for the dry cooler and the pump in the primary side of the CDU, as illustrated in Fig. 13.

As previously stated, Scheme 1 recovers waste heat from the secondary side of the CDU (refer to Fig. 5). In this configuration, the pump on the primary side of the CDU is activated only when surplus waste heat is available. In contrast, Scheme 2 recovers waste heat from the primary side of the CDU (see Fig. 6), which requires continuous operation of the pump on the primary side of the CDU. Therefore, during the winter season in January, February, and December, the electricity inputs for the dry cooler and pump in the primary side of CDU are reduced to zero for Scheme 1. Overall, compared to the base case, Schemes 1 and 2 yield yearly electricity savings of 2290.5 and 905.2 kWh, respectively. Based on the electricity prices listed in Table 3, these savings amount to 276 € and 109 € per year for Schemes 1 and 2, respectively. Given the limited liquid cooling capacity of 25 kW for the WSTAR data center, these savings hold significant importance from an energy efficiency perspective, especially in Scheme 1, where approximately 1% of the cooling capacity (25 kW) is conserved.

Scheme 1 outperforms Scheme 2 in terms of waste heat recovery and electricity savings. The extent of this superiority depends on the setting of the rack inlet coolant temperature. Generally, the gap widens as the rack inlet coolant temperature decreases. Thus, from both safety and energy perspectives, Scheme 1 emerges as the superior choice.

Although the impact of heat exchanger effectiveness (HX2 and CDU_HX) on the two schemes' performance is not studied in this work, it is evident that the performance gap between the schemes diminishes with increasing effectiveness. However, higher effectiveness for a plate heat exchanger can result in fouling, increased pressure drops, higher costs, and additional maintenance. Thus, considering maintenance and operation, Scheme 1 is also an optimal selection.

Despite the thorough exploration of the proposed innovative solutions, it is important to acknowledge that there are limitations and potential exclusions in the application of the developed schemes, which are described as follows:

- The developed schemes exhibit reduced efficiency when applied in high-temperature heating systems, especially Scheme 2. For instance, in old existing buildings where the maximum supply and return water temperatures on the secondary side of the space heating network are set at 70 °C and 40 °C, respectively [30], this 40 °C return water temperature is 10 °C higher than the new regulation. Such elevated return water temperatures significantly reduce the temperature difference between the hot and cold fluids for heat recovery heat exchanger HX2, leading to an insufficient heat exchange rate during cold weather.
- The developed schemes are less effective in a liquid cooling system with a constant flow rate on the secondary side of the CDU. The reason mirrors the first limitation. If the flow rate remains constant on the secondary side of the CDU, the rack outlet coolant temperature decreases during partial loads, resulting in a reduction of the temperature difference between the hot and cold fluids for heat recovery heat exchanger HX2.
- Both schemes are specifically designed for distributed and edge data centers situated within buildings. Standalone data centers require further investigation, which could be a focus for future research.

3.2. Life cycle cost and CO_2 emission reductions

Figs. 14–15 present the LCC and CO_2 emission reductions for the proposed two schemes.

The payback period for both schemes is less than one year, indicating their profitability from the perspective of the building owner. Over a span of 25 years, Scheme 1 is estimated to save approximately 203,287€ in district heating costs compared to the base case, while Scheme 2 is expected to save about 177,443€. Notably, Scheme 1 demonstrates an additional saving of 25,844 € compared to Scheme 2. Importantly, both Schemes 1 and 2 contribute to a significant reduction in CO_2 emissions, with total reductions of 291,996 $kgCO_2$ and 258,192 $kgCO_2$, respectively.

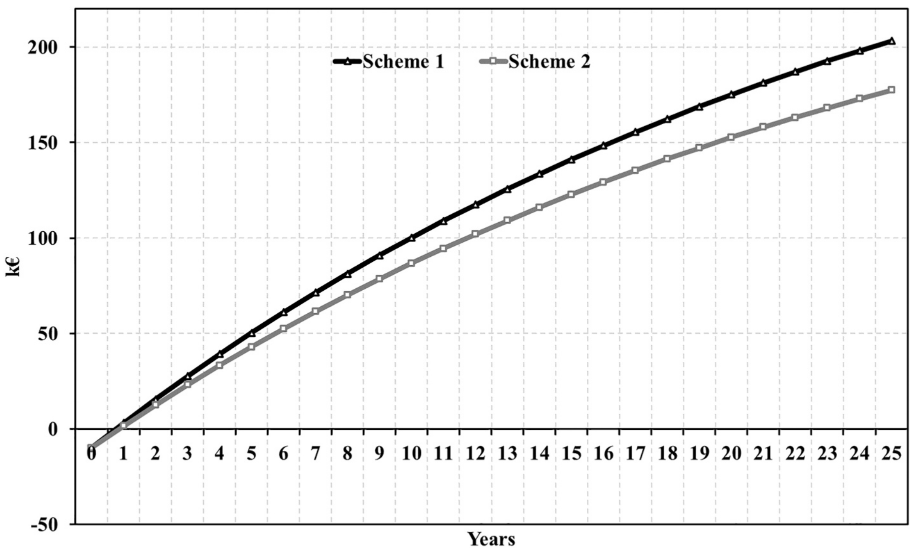

Fig. 14. NPV for life cycle cost savings.

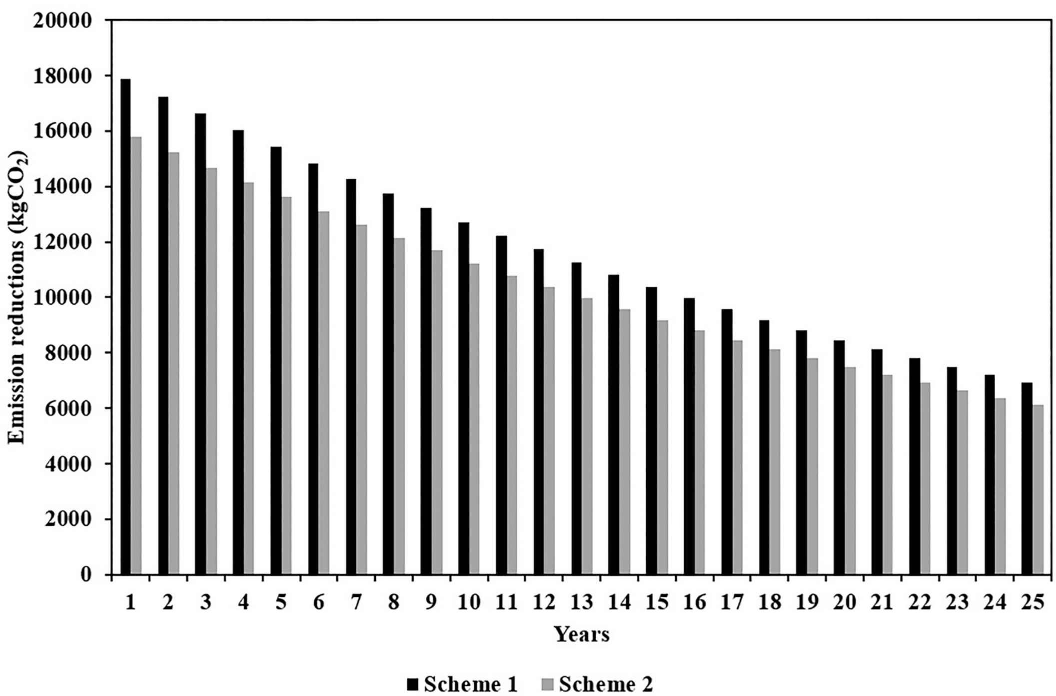

Fig. 15. Life cycle CO_2 emission reductions.

Conducting LCC analysis that accounts for the impact of climate change is particularly challenging because of the limitations in obtaining reliable projected climate data. A study [54] conducted in Finland reveals a significant trend: the annual heating demand for buildings is expected to decrease by 2–4% per decade, while the annual cooling demand is projected to increase by 4–8% per decade. This projected result translates to a potential 5–10% reduction in heating demand for the building after 25 years. Consequently, the recovered waste heat will decrease, resulting in reduced profitability and longer payback times for both schemes. Notably, Scheme 2's waste heat recovery rate decreases as outdoor temperatures drop (as illustrated in Fig. 10). This means that Scheme 2 benefits from milder winters, which narrows the performance gap between the two schemes. However, as demonstrated in Fig. 11, during cold months, the building's heating demands greatly exceed the available waste heat capacity. Consequently, a 5–10% reduction in heating demands has a relatively minor impact on the recovered waste heat for both schemes. This results in a higher percentage of reused waste heat in meeting heating energy needs, signifying a more renewable heating energy source for the building. It is essential to recognize that the discussions presented here are based on limited climate change resources, and a more comprehensive study is necessary in the future to substantiate and quantify these findings.

While uncertainties exist in LCC analysis, all the results presented in this paper clearly demonstrate that, from both an economic and CO_2 emission perspective, Scheme 1 outperforms Scheme 2. Crucially, both schemes exhibit a payback time of less than a year due to their low initial investment cost and system energy consumption.

4. Conclusions and future work

Two heat exchanger design schemes, Scheme 1 and Scheme 2, are proposed to directly utilize data center waste heat from a liquid-cooled rack for the building space heating network. Scheme 1 recovers waste heat from the secondary side of CDU, while Scheme 2 recovers waste heat from the primary side. Using TRNSYS 18, we thoroughly study their waste heat utilization rate performance and quantify the recovery potentials for both primary and secondary sides, making this the pioneering paper on such a study for liquid-cooled data centers. Further, we conduct analyses on LCC and CO_2 emission reduction for both schemes.

The findings of our study are carefully presented and discussed in Section 3. The following conclusive results can be reached:

- Initially, we believed that high-grade waste heat from liquid-cooled data centers could be fully recovered and reused when building heating demand surpasses waste heat. However, our simulations reveal a different reality. The results indicate that connecting the heat recovery heat exchanger to the primary side of CDU (Scheme 2) leads to a decrease in the waste heat recovery rate as the outdoor temperature drops. On the contrary, connecting the heat exchanger to the secondary side of CDU (Scheme 1) avoids this issue and maintains a constant waste heat recovery rate, regardless of outdoor temperature. This crucial finding represents one of the major contributions of this paper, which highlights the importance for designers of data center waste heat utilization systems to consider not only rack inlet coolant temperature, coolant flow rate, and facility flow rate but also the connection side of CDU for heat recovery heat exchangers.
- Both schemes can achieve profitability within one year due to the absence of a heat pump requirement, leading to significant reductions in investment, energy and CO_2 emission.
- Both schemes substantially decarbonize the data center and the building space heating network by reducing district heating and electricity consumption.

These new findings result from multiple novelties developed in this paper. Notably, it is the first research paper to examine liquid cooling waste heat recovery system performance for DH-based building space heating network on the primary and secondary sides of a CDU. The common practice is to use heat pumps, but our proposed method eliminates the need for a heat pump, resulting in significant energy and CO_2 emission savings. A novel relationship graph between waste heat recovery rate and outdoor temperature is introduced to aid and optimize system design. Analyzing these graphs reveals that waste heat recovery rate may decrease with outdoor temperature when recovering waste heat from the primary side of a CDU in colder weather, which presents a completely new discovery that will impact future carbon-neutral data center designs.

Limitations exist despite the comprehensive scope of this study. One limitation of this work is the absence of waste heat utilization on the air-cooled electronic components and racks (approximately 25 kW) due to the undetermined cooling method—whether to use direct evaporative cooling or develop a new approach. Consequently, crucial research on topics such as the impact on Power Usage Effectiveness (PUE) when reusing waste heat and the potential Energy Reuse Effectiveness (ERE) remains unexplored. In future studies, incorporating air-cooled electronic components for waste heat utilization will allow us to investigate these significant areas. A simple and effective approach would be to employ a run-around heat recovery system [55] to recover waste heat from the hot exhaust air dissipated by air-cooled electronic components and racks. This system can preheat outdoor air for building air handling units (AHU) during winter, preventing AHU heat recovery units from freezing and enhancing efficiency under extreme cold conditions. Additionally, we will examine the impact of the run-around heat recovery system's location on waste heat reuse, while comparing its life cycle cost and CO_2 emission reductions with those of a heat pump heat recovery system.

Another limitation is the uncertainty associated with the projected climate data, which may affect the accuracy of our detailed LCC analysis regarding climate change impact issues, as discussed earlier. This topic will be also our future study.

Another noteworthy area of future research is investigating the full recovery of data center waste heat under extreme cold weather conditions (e.g., $<-20\,^{\circ}C$) from the primary side of CDU without significantly increasing the heat exchanger effectiveness. This is crucial as recovering waste heat from the primary side is more common.

CRediT authorship contribution statement

Tao Lu: Writing – original draft, Methodology, Data curation, Conceptualization. **Xiaoshu Lü:** Writing – review & editing, Supervision, Methodology, Funding acquisition, Conceptualization. **Petri Välisuo:** Writing – review & editing, Supervision, Funding acquisition. **Qunli Zhang:** Writing – review & editing, Investigation. **Derek Clements-Croome:** Writing – review & editing, Investigation.

Declaration of Competing Interest

The authors declare that they have no known competing financial interests or personal relationships that could have appeared to influence the work reported in this paper.

Data availability

Data will be made available on request.

Acknowledgement

This project has received funding from the European Union - NextGenerationEU instrument and is funded by the Academy of Finland under grant number No 353562.

References

[1] International Energy Agency. https://www.iea.org/fuels-and-technologies/data-centres-networks (accessed on 22 Jun 2923).
[2] Finland Ministry of the Environment, Government's climate policy: climate-neutral Finland by 2035, https://ym.fi/en/climate-neutral-finland-2035, (accessed on 22 Jun 2923).
[3] Wikipedia. Green data center. https://en.wikipedia.org/wiki/Green_data_center (accessed on 22 Jun 2923).
[4] Lu T, Lü X, Remes M, Viljanen M. Investigation of air management and energy performance in a data center in Finland: case study. Energ Buildings 2011;43: 3360–72. https://doi.org/10.1016/j.enbuild.2011.08.034.
[5] Wahlroos M, Pärssinen M, Rinne S, Syri S, Manner J. Future views on waste heat utilization – case of data centers in northern Europe. Renew Sustain Energy Rev 2018;82:1749–64. https://doi.org/10.1016/j.rser.2017.10.058.
[6] IEA. Heating. https://www.iea.org/energy-system/buildings/heating.
[7] Paiho S, Saastamoinen H. How to develop district heating in Finland? Energy Policy 2018;122:668–76. https://doi.org/10.1016/j.enpol.2018.08.025.
[8] Statistics Finland, Energy and emissions, (accessed on 22 Jun 2923).
[9] The Ministry of the Environment of Finland. Method for the whole life carbon assessment of buildings. Publications of the Ministry of the Environment; 2019.
[10] Lund H, Möller B, Mathiesen BV, Dyrelund A. The role of district heating in future renewable energy systems. Energy 2010;35:1381–90. https://doi.org/10.1016/j.energy.2009.11.023.
[11] Lindroos TJ, Mäki E, Koponen K, Hannula I, Kiviluoma J, Raitila J. Replacing fossil fuels with bioenergy in district heating – comparison of technology options. Energy 2021;231:120799. https://doi.org/10.1016/j.energy.2021.120799.
[12] DataCenterKnowledge. Sea-Cooled Data Center Heats Homes in Helsinki. https://www.datacenterknowledge.com/archives/2011/09/06/sea-cooled-data-center-heats-homes-in-helsinki#close-modal (accessed on 23 Jun 2923).
[13] Motiva. Energy efficiency of data centers in Finland, Reoprt. 2022.
[14] Fortum. Fortum and Microsoft's data centre project advances climate targets. https://www.fortum.com/data-centres-helsinki-region (accessed on 23 Jun 2923).
[15] Oróa E, Taddeob P, Salomb J. Waste heat recovery from urban air cooled data centres to increase energy efficiency of district heating networks. Sustain Cities Soc 2019;45:522–42. https://doi.org/10.1016/j.scs.2018.12.012.

[16] Oltmanns J, Sauerwein D, Dammel F, Stephan P, Kuhn C. Potential for waste heat utilization of hot-water-cooled data centers: a case study. Energy Sci Eng 2020;8: 1793–810. https://doi.org/10.1002/ese3.633.
[17] He Z, Ding T, Liu Y, Li Z. Analysis of a district heating system using waste heat in a distributed cooling data center. Appl Therm Eng 2018;141:1131–40. https://doi.org/10.1016/j.applthermaleng.2018.06.036.
[18] Deymi-Dashtebayaz M, Valipour-Namanlo S. Thermoeconomic and environmental feasibility of waste heat recovery of a data center using air source heat pump. J Clean Prod 2019;219:117–216. https://doi.org/10.1016/j.jclepro.2019.02.061.
[19] Yu J, Jiang Y, Yan Y. A simulation study on heat recovery of data center: a case study in Harbin, China. Renew Energy 2019;130:154e173. https://doi.org/10.1016/j.renene.2018.06.067.
[20] Zhang P, Wang B, Wu W, Shi W, Li X. Heat recovery from internet data centers for space heating based on an integrated air conditioner with thermosyphon. Renew Energy 2015;80:396–406. https://doi.org/10.1016/j.renene.2015.02.032.
[21] Deymi-Dashtebayaz M, Namanlo SV, Arabkoohsar A. Simultaneous use of air-side and water-side economizers with the air source heat pump in a data center for cooling and heating production. Appl Therm Eng 2019;161:114133.
[22] Norani M, Deymi-Dashtebayaz M. Energy, exergy and exergoeconomic optimization of a proposed CCHP configuration under two different operating scenarios in a data center: case study. J Clean Prod 2022;342:130971.
[23] Alipour M, Deymi-Dashtebayaz M, Asadi M. Investigation of energy, exergy, and economy of co-generation system of solar electricity and cooling using linear parabolic collector for a data center. Energy 2023;279:128076.
[24] Douchet F, Nortershauser D, Le Masson S, Glouannec P. Experimental and numerical study of water-cooled datacom equipment. Appl Therm Eng 2015;84: 350–9. https://doi.org/10.1016/j.applthermaleng.2015.03.030.
[25] Nada SA, El-Zoheiry RM, Elsharnoby M, Osman OS. Experimental investigation of hydrothermal characteristics of data center servers' liquid cooling system for different flow configurations and geometric conditions. Case Stud Therm Eng 2021;27:101276. https://doi.org/10.1016/j.csite.2021.101276.
[26] Zimmermann S, Meijer I, Tiwari MK, Paredes S, Michel B, Poulikakos D. Aquasar: a hot water cooled data center with direct energy reuse. Energy 2012;43:237–45. https://doi.org/10.1016/j.energy.2012.04.037.
[27] Khalaja AH, Halgamuge SK. A review on efficient thermal management of air- and liquid-cooled data centers: from chip to the cooling system. Appl Energy 2017;205: 1165–88. https://doi.org/10.1016/j.apenergy.2017.08.037.
[28] Hnayno M, Chehade A, Klaba H, Bauduin H, Polidori G, Maalouf C. Performance analysis of new liquid cooling topology and its impact on data centres. Appl Therm Eng 2022;213:118733. https://doi.org/10.1016/j.applthermaleng.2022.118733.
[29] Coles H, Greenberg S. Direct Liquid Cooling for Electronic Equipment. Berkeley Lab, US: Report; 2014.
[30] Publication K1/2021. Rakennusten kaukolämmitys-Määräykset ja Ohjeet-Julkaisu K1/2021(District Heating of Buildings-Regulations and Guidelines-Publication K1/2021), Energiateollisuus. https://lnkd.in/gsyNvwk2 (accessed on 26 June 2023). (in Finnish).
[31] Taddeo P. Waste heat recovery from urban data centres and reuse to increase energy efficiency of district heating and cooling network. Master thesis,. Spain, Barcelona: Universitat Politècnica de Catalunya; 2017.
[32] https://wstardatacenter.fi/about/ (accessed on 26 June 2023).
[33] The Future of Data Centers: Distributed, Grid or Cloud Computing?. https://www.datacenters.com/news/future-data-centers-distributed-grid-or-cloud-computing (accessed on 26 June 2023).
[34] Gillis AS. edge data center, Techtarget. https://www.techtarget.com/searchdatacenter/definition/edge-data-center.
[35] Eleanor Jane D, Fatme E. Utilising waste heat from Edge-computing Micro Data Centres: Financial and Environmental synergies, Opportunities, and Business Models, Thesis, KTH, Sweden. 2021.
[36] TRNSYS 18 documentation, mathematical reference. University of Wisconsin-Madison; 2019.
[37] Kadhim MA. Holistic study of thermal Management in Direct Liquid Cooled Data Centres: From the Chip to the environment. Doctoral dissertation,. University of Leeds; 2018.
[38] ASHRAE. Liquid Cooling Guidelines for Datacom Equipment Centers. Atlanta, GA: American Society of Heating, Refrigeration and Air-Conditioning Engineers; 2014.
[39] Asetek. Installation operation & maintenance guide InRackCDU (4U-V2). Asetek manual; 2019.
[40] Airedale Dry. Coolers - DR10-DR95, dry coolers technical manual 9308503, Leeds, UK. 2018.
[41] O'Neal D, Edmondson JL, Yi P. Comparison of performance characteristics of SCR and ECM controlled series fan powered terminal units. HVAC&R Res 2014;20: 194–202. https://doi.org/10.1080/10789669.2013.850959.
[42] ATS. Calculating the loads for liquid cooling systems. Norwood. MA. USA: Advanced Thermal Solution, Inc; 2023.
[43] TRNSYS 18 Documentation. HVAC library mathematical reference. University of Wisconsin-Madison; 2019.
[44] Ju Y, Jokisalo J, Kosonen R. Peak shaving of a district heated office building with short-term thermal energy storage in Finland. Buildings 2023;13:573. https://doi.org/10.3390/buildings13030573.
[45] Laitinen A, Tuominen P, Holopainen R, Tuomaala P, Jokisalo J, Eskola L, et al. Renewable energy production of Finnish heat pumps - final report of the SPF-project. VTT Technol 2014;164.
[46] nVent. Rack Level High Density Liquid Cooling, White paper. 2019.
[47] CooLIT. Rack DCLCTM product guide, CooLIT systems. 2023.
[48] Gluch P, Baumann H. The life cycle costing (LCC) approach: a conceptual discussion of its usefulness for environmental decision-making. Build Environ 2004;39:571–80. https://doi.org/10.1016/j.buildenv.2003.10.008.
[49] Dzhigit T. Heating system for a passive house in Finland. Bachelor's thesis,. Finland: Mikkeli University of Applied Sciences; 2012.
[50] Pulakka S. Life-cycle cost methods and tools, in: Proceedings of 9th international conference on durability of building materials and components. Australia: Brisbane; 2002.
[51] One Click LCA®. Automate building life cycle cost calculations. https://www.oneclicklca.com/construction/life-cycle-costing-software/; 2023 (accessed on 15 Jun 2023).
[52] Statistics Finland. Tilastokeskus. https://pxdata.stat.fi/PxWeb/pxweb/en/StatFin/StatFin_ehi/; 2023 (accessed on 15 Jun 2023).
[53] Finnish Ministry of the Environment. Method for the whole life carbon assessment of buildings. Publications of the Ministry of the Environment; 2019.
[54] Jylhäa K, Jokisalo J, Ruosteenoja K, Pilli-Sihvola K, Kalamees T, Seitolaa T, et al. Energy demand for the heating and cooling of residential houses in Finland in a changing climate. Energ Buildings 2015;99:104–16. https://doi.org/10.1016/j.enbuild.2015.04.001.
[55] Lu T, Lü X, Kibert C, Puttonen J. The application of linear regression and the power law relationship of air-side heat transfer with field measurements to model the performance of run-around heat recovery systems. Energ Buildings 2016;110: 453–67. https://doi.org/10.1016/j.enbuild.2015.10.028.